Search, Map, and Analyze the Dynamics of Fragile Geologic Features

Project objectives

Earthquake geology provides constraints on ground rupture and ground motions from Southern California's faults over sufficiently long time scales that most available earthquake sources have been activated. These data are complementary to geodetic and seismological records. However, the epistemic uncertainties from earthquake geology data remain high. This is certainly true for FGFs applied to seismic hazards. The SCEC Earthquake Geology research strategies include "Analysis and dating of precariously balanced rocks and other fragile geologic features to evaluate ground motion hazard and inform seismic hazard methodologies." Priorities include developing data sets of fragile geologic features and refining fragility analysis. At the 2019 SCEC annual meeting, renewed interest in FGFs was evident in the Workshop on Evaluation of Seismic Hazard Models with Fragile Geologic Features (https://www.scec.org/workshops/2019/FGF). Key issues included single- vs. multi-PBR fragility models and FGF evaluation in a diversity of geomorphic settings. Our proposed work was inspired by these discussions.

We developed a pipeline for identifying and then mapping PBRs at close range. We also studied the feasibility of dynamical studies in a physics engine. By combining methodology for mapping PBRs for stability trait characterization, and exploring simplified PBR dynamics through simulation studies, we advanced a comprehensive understanding of PBR sites and geologic factors affecting them, decreasing epistemic uncertainty for their seismic hazard contributions.

Robotic mapping is useful in scientific applications that involve surveying unstructured environments. This paper presents a target-oriented mapping system for sparsely distributed geologic surface features, such as precariously balanced rocks (PBRs), whose geometric fragility parameters can provide valuable information on earthquake shaking history and landscape development for a region. With this geomorphology problem as the test domain, we demonstrate a pipeline for detecting, localizing, and precisely mapping fragile geologic features distributed on a landscape. To do so, we first carry out a lawn-mower search pattern in the survey region from a high elevation using an Unpiloted Aerial Vehicle (UAV). Once a potential PBR target is detected by a deep neural network, we track the bounding box in the image frames using a real-time tracking algorithm. The location and occupancy of the target in world coordinates are estimated using a sampling-based filtering algorithm, where a set of 3D points are re-sampled after weighting by the tracked bounding boxes from different camera perspectives. The converged 3D points provide a prior on 3D bounding shape of a target, which is used for UAV path planning to closely and completely map the target with Simultaneous Localization and Mapping (SLAM). After target mapping, the UAV resumes the lawn-mower search pattern to find the next target. We introduce techniques to make the target mapping robust to false positive and missing detection from the neural network. Our target-oriented mapping system has the advantages of reducing map storage and emphasizing complete visible surface features on specified targets.

Methodology

Details of our methodology has been submitted to the IEEE Robotics and Automation Letters.

Fig. 1: (Top left) A precariously balanced rock (PBR) in Granite Dells, Arizona. (Bottom left) Reconstructed world in Gazebo. (Right) Resulting mapped PBR from the reconstructed scene.

The proposed target-oriented mapping system is composed of a perception subsystem (Fig. 2) and a motion subsystem (Fig. 3). We start by carrying out a lawn-mower search pattern in the survey region from a high elevation using a UAV. Once a potential PBR target is detected by a deep neural network, we track the target bounding box in image coordinates using a bounding box tracking algorithm. We generate 3D points from the tracked bounding box and resample them with our sampling-based filtering algorithm. When the 3D points are assessed to be converging, the UAV employs a circular motion at the same search elevation to keep filtering 3D points. A bounding cylinder (b-cylinder) is then constructed from the converged 3D points for UAV path planning to closely and completely map the target with SLAM. After target mapping, the UAV resumes the lawnmower search pattern to find the next target.

The perception subsystem workflow is shown in Fig. 2. We deploy two tracking modules: one for bounding boxes and one for 3D points. The bounding box tracking module subscribes to detection messages from a neural network and publishes tracked bounding boxes to the 3D points tracking module. The essence of the 3D points tracking module is a sampling-based filtering algorithm where a set of 3D points are re-sampled after weighting by the tracked bounding boxes from different camera perspectives (see Sec. IV B). We construct a b-cylinder from the converged 3D points and conduct close and complete target mapping with SLAM.

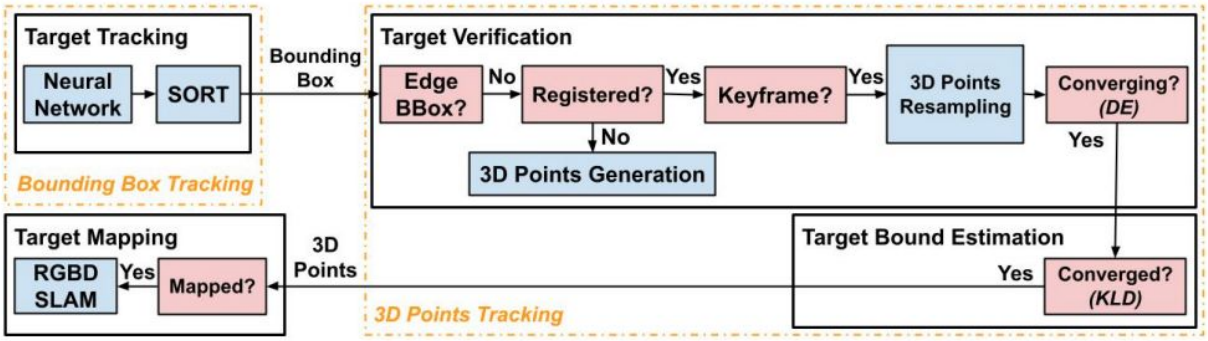

Fig. 2: Perception subsystem workflow.

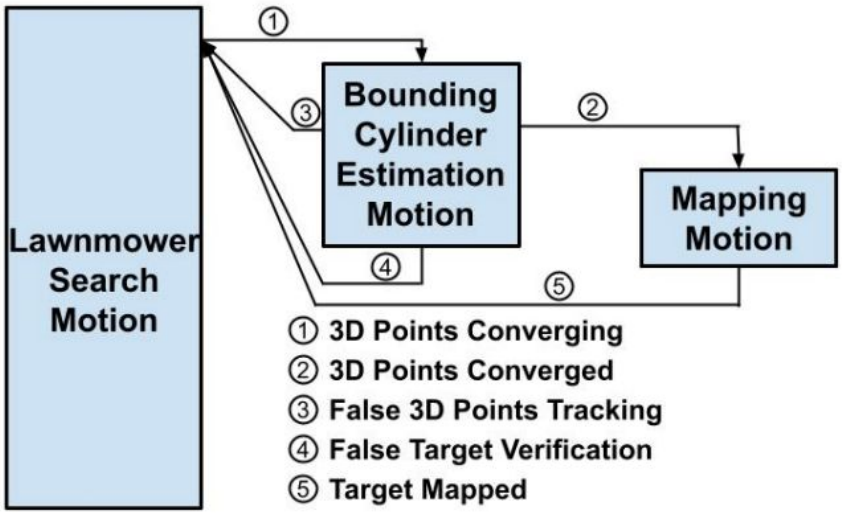

(a) Motion state diagram

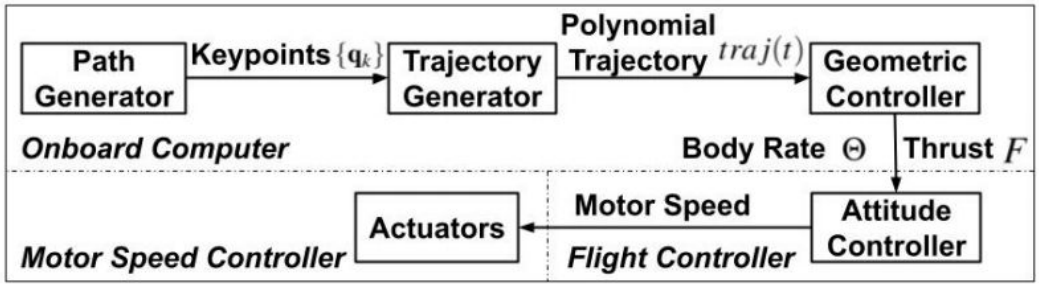

(b) Controller workflow

Fig. 3: Motion subsystem.

Results obtained

We evaluated the target-oriented mapping system with two experiments in Gazebo simulation using a gaming laptop, Dell G7: Intel Core i7-8750H, 16GB RAM, and Nvidia GeForce GTX 1060 Max-Q, which has similar computing capacity with Intel NUC i7 plus Nvidia TX2. In both experiments, we use a 3DR Iris with an RGBD sensor ($\gamma = 60°$) operated by PX4 SITL and MAVROS. The UAV pose estimation is maintained by an EKF fusing data from IMU in the flight controller and a GPS module. Sensor noises of GPS, IMU, and magnetometer are also simulated in Gazebo. A tiny YOLO v2 is initialized from the darknet53 [21] and finely tuned with the images collected in the Gazebo worlds, and the real-time inference is deployed using YOLO ROS [22]. We apply RTAB-MAP [9] for RGBD mapping, and the mapping service is only activated during the mapping motion. The vertical scanning field of view β is 40°. For the control system, the maximum velocity is 1m/s and the maximum acceleration is 1m/s 2 . The first experiment is conducted to demonstrate the target-oriented mapping pipeline for a field reconstructed from real data. We built the mesh model with one PBR (Fig. 1 (bottom left)) using SfM with UAV imagery that was manually collected at Granite Dells, Prescott AZ, 2019. The UAV trace with different motion states is shown in Fig. 6a. As the mapping result presented in Fig. 1 (right), the presented system has mapped the target and also provided access to the complete visible surface features of the PBR including the ground basal contact, which is crucial to calculate the PBR's fragility for earthquake studies.

The purpose of the second experiment is to examine the system with multiple sparsely distributed targets. The 3D terrain model (Fig. 7a) is built in Blender [23] with texture from satellite imagery and digital elevation model from OpenTopography [24]. We import seven synthesized PBRs to the terrain model as our mapping targets. The UAV trace is shown in Fig. 6b, and the mapping results are displayed in Fig. 7b. We show the system robustness by measuring the performances of key components in Experiment II (Table. I). As false positive and missing detections are the major cause of the problems in the following components, we inspect the worst neural network detection performance (IoU>0.5) in one of the seven PBR mappings, where each begins from the end of a previous PBR mapping to the converged assessment of a current PBR. The other components are measured for the entire seven PBR mappings based on the target states presented from the system and the desired target states without considering mission duration. For the false positives and false negatives of converging, we only consider the cases that are caused by false detections from the neural network. We neglect the cases where there are not enough detections due to the bounding box is too close to the image edges, because they are eventually detected from other search perspectives. This experiment shows the robustness of the system as all seven PBRs are successfully mapped, especially with regard to the existence of false positives and false negatives in other components.

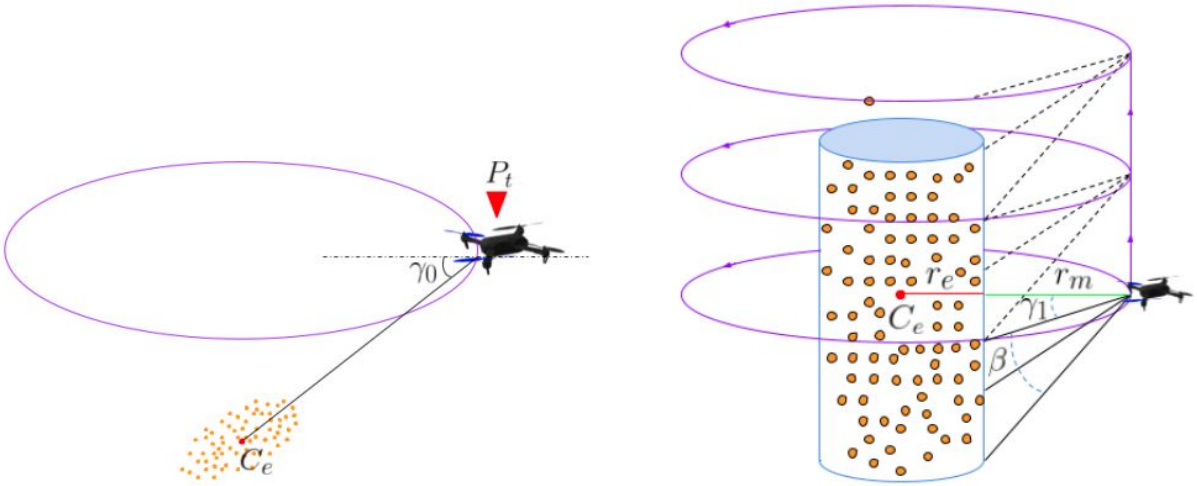

(a) View planning for b-cylinder estimation

(b) View planning for target mapping

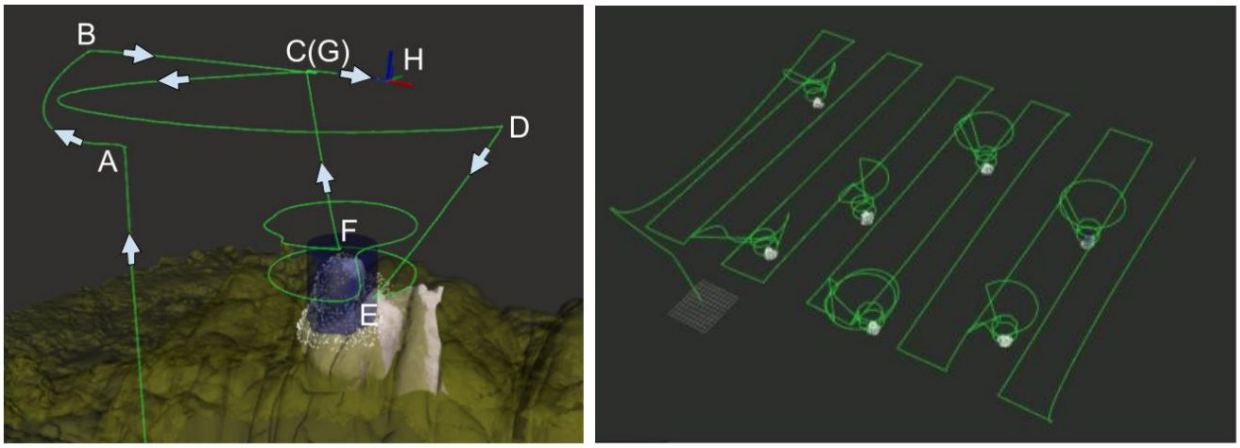

(a) UAV trace of Experiment I.

(b) UAV trace of Experiment II.

Fig. 6: UAV traces. (a) $\overline{ABC}$ is lawn-mower search trace. $\overline{CD}$ is b-cylinder estimation motion trace, and target is assessed as converging at C and as converged at D. $\overline{EF}$ is the target mapping trace. $\overline{GH}$ is resumed lawn-mower search trace.

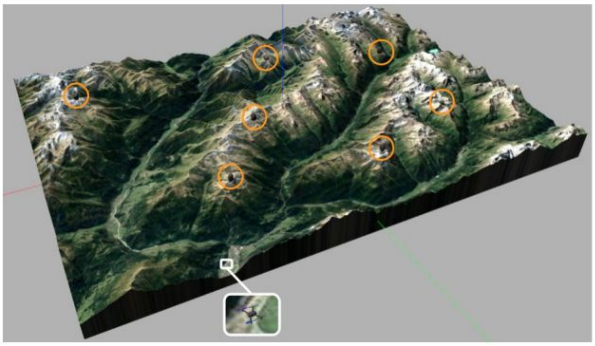

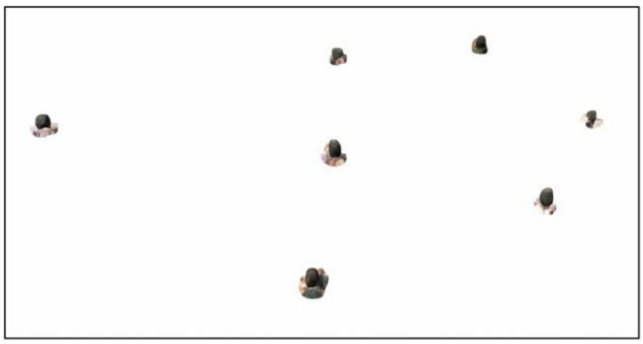

(a) Gazebo world for Experiment II (b) Mapping results

Fig. 7: Gazebo world and mapping results from Experiment II.

TABLE I: Target-oriented Mapping System Performance

	worst	all			
	detection	generation	converging	converged	mapped
precision	88.7%	84.6%	88.9%	100%	100%
recall	78.3%	100%	100%	87.5%	100%

Analysis framework

To analyze rocks mapped using our search and map pipeline, we developed a framework by teaming up with Prof. Christine Wittich at University of Nebraska-Lincoln. In this framework, are connecting our proposed pipeline leveraging physics engines, with prior methods for fragility analysis of precariously balanced rocks. As a result, we were able to start using shake properties and metrics defined with prior principled methods, into the arena of discrete element modeling in physics engines such as those deployed in our OpenUAV simulation testbed. Preliminary results are promising, showing insights into the PGA vs PGV/PGA relationships, and toppling probability.

Fig. 8 shows a screenshot of one of our analysis videos available at https://www.youtube.com/watch?v=Edt7oGTkscM

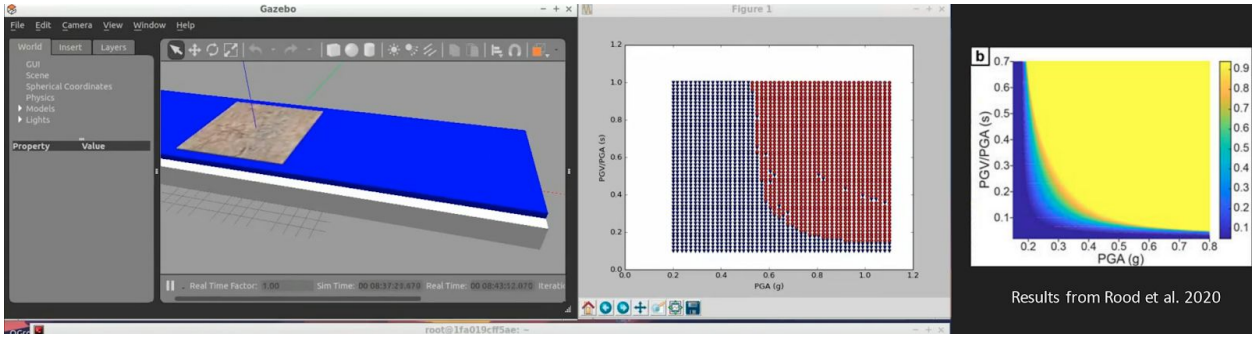

Fig 8: Comparison of results from discrete element modeling in Gazebo simulator, with solutions using principled methods established by Rood et al. 2020.

Conclusions:

Our SCEC work developed a target-oriented system for UAV to map fragile geologic features such as PBRs, whose geometric fragility parameters can provide valuable information on earthquake processes and landscape development. Such a system provides access to autonomous PBR mapping, which was lacking in field geology but will be essential to geologic model assessment. Our ultimate goal is to deploy this target-oriented mapping system to actual boulder fields and to assess the quality of 3D mapping. Additionally, 3D semantic segmentation should be applied to extract 3D points of PBRs from their contact terrains, which leads to PBR surface reconstruction. We have implemented the circular motion for target mapping, which is based on an assumption that there are no obstacles during the mapping. This can be improved by framing the mapping task as a probabilistic exploration problem. Next-bestview or frontier-based exploration algorithms [25, 26] can be used to generate an obstacle-free path and accurately determine occupancy within the bounding cylinder.

References

[1] J. N. Brune. “Precariously balanced rocks and ground motion maps for Southern California”. In: Bulletin of the Seismological Society of America 86.1A (1996), pp. 43–54.

[2] A. Anooshehpoor, J. N. Brune, and Y. Zeng. “Methodology for obtaining constraints on ground motion from precariously balanced rocks”. In: Bulletin of the Seismological Society of America 94.1 (2004), pp. 285–303.

[3] D. E. Haddad, O. Zielke, J. R. Arrowsmith, M. D. Purvance, A. G. Haddad, and A. Landgraf. "Estimating two dimensional static stabilities and geomorphic settings of precariously balanced rocks from unconstrained digital photographs". In: Geosphere 8.5 (2012), pp. 1042–1053.

[4] C. E. Wittich, T. C. Hutchinson, J. DeSanto, and D. Sandwell. "3D reconstructions and numerical simulations of precarious rocks in Southern California". In: (2018).

[5] D. E. Haddad, S. O. Akçiz, J. R. Arrowsmith, D. D. Rhodes, J. S. Oldow, O. Zielke, N. A. Toké, A. G. Haddad, J. Mauer, and P. Shilpakar. "Applications of airborne and terrestrial laser scanning to paleoseismology". In: Geosphere 8.4 (2012), pp. 771–786.

[6] K. Johnson, E. Nissen, S. Saripalli, J. R. Arrowsmith, P. McGarey, K. Scharer, P. Williams, and K. Blisniuk. "Rapid mapping of ultrafine fault zone topography with structure from motion". In: Geosphere 10.5 (2014), pp. 969–986.

[7] Z. Chen, T. R. Scott, S. Bearman, H. Anand, D. Keating, C. Scott, J. R. Arrowsmith, and J. Das. "Geomorphological analysis using unpiloted aircraft systems, structure from motion, and deep learning". In: 2020 IEEE/RSJ International Conference on Intelligent Robots and Systems (IROS). 2020, pp. 1276–1283.

[21] J. Redmon and A. Farhadi. "YOLO9000: better, faster, stronger". In: Proceedings of the IEEE conference on computer vision and pattern recognition. 2017, pp. 7263–7271. [22] M. Bjelonic. YOLO ROS: Real-time object detection for ROS. https : / / github . com / leggedrobotics / darknet_ros. 2018.

[23] B. O. Community. Blender - a 3D modelling and rendering package. Blender Foundation. Stichting Blender Foundation, Amsterdam, 2018. URL: http://www.blender.org.

[25] A. Bircher, M. Kamel, K. Alexis, H. Oleynikova, and R. Siegwart. "Receding horizon "next-best-view" planner for 3D exploration". In: IEEE International Conference on Robotics and Automation (ICRA). 2016, pp. 1462–1468.

[26] S. Song and S. Jo. "Surface-based exploration for autonomous 3D modeling". In: 2018 IEEE International Conference on Robotics and Automation (ICRA). IEEE. 2018, pp. 4319–4326.